

71

## Ultrasonic Assessment of Skin and Wounds With the Scanning Laser Acoustic Microscope

John E. Olerud, M.D., William O'Brien, Jr., Ph.D., Mary Ann Riederer-Henderson, Ph.D., Diane Steiger, M.S., Fred K. Forster, Ph.D., Colin Daly, Ph.D., Deborah J. Ketterer, B.S., and George F. Odland, M.D.

Departments of Medicine (Dermatology) (JEO, GFO), Orthopaedics (Sports Medicine) (JEO), Biological Structure (GFO), and Mechanical Engineering (FKF, CD), University of Washington, Seattle; Department of Orthopaedics, University of Washington and Veterans Administration Medical Center (MAR-H, DJK), Seattle, Washington; Department of Electrical and Computer Engineering, University of Illinois (WO'B, DS), Urbana, Illinois, U.S.A.

The aim of the present study was to test the hypothesis that ultrasonic propagation properties in skin and wound tissue would correlate with material properties such as collagen content, water content, and tensile strength of those tissues. Both ultrasonic speed and ultrasonic attenuation coefficient were directly correlated with tissue collagen content, [ $r = 0.80$  and  $r = 0.56$ , respectively ( $p < 0.001$ )]. In addition, ultrasonic speed and attenuation coefficient were inversely correlated with tissue water content, [ $r =$

$-0.57$  and  $r = -0.73$ , respectively ( $p < 0.001$ )]. Tensile strength also correlated very significantly with ultrasonic speed ( $r = 0.90$ ,  $p < 0.001$ ), and significantly with attenuation coefficient ( $r = 0.58$ ,  $p < 0.001$ ). The results demonstrate the feasibility of using ultrasound for noninvasively determining the material properties of biologic tissues including healing cutaneous wounds. *J Invest Dermatol* 88: 615-623, 1987

**T**he study of human wounds is limited by the lack of a generally applicable method permitting objective assessment of wounds in a noninvasive manner. Classic methodologies utilized in wound healing research such as tensile strength testing, collagen biochemistry, and morphology require some degree of wound disruption [1]. This consideration alone restricts the use of such methods in the study of human wounds.

Ultrasound is an investigative tool with widespread clinical application in the noninvasive evaluation of organs including brain, liver, spleen, kidneys, heart, and major blood vessels [2]. In conventional systems, ultrasonic energy at frequencies ranging from 1-10 MHz is used for imaging target organs. Recently, a higher frequency ultrasonic system (25-50 MHz) has been described for imaging the skin [3]. An increase in the ultrasonic frequency results in an increase in the image resolution. Feasibility of measuring skin thickness in various abnormal states such as scleroderma and steroid-induced thinning of the skin has been shown with this high-frequency system. In addition, the boundaries of certain tumors of the skin were delineated. The superficial nature

of the skin facilitates the use of higher-frequency ultrasound since the ultrasonic attenuation of skin and other intervening tissues on the wave path to deeper target organs is not a limiting factor.

Clinical ultrasonic images are created by the backscatter of ultrasound energy from discontinuities wherever acoustic propagation properties in tissues are sufficiently different. In addition to creating images by displaying echo patterns, it is possible to use ultrasound properties such as wave speed and attenuation coefficient to assess material properties of tissues. These measurements of material properties contain information regarding tissue composition and mechanical characteristics. In the present study, such a fundamental approach was taken to gain information regarding the material properties of skin and experimentally produced wounds. We used a scanning laser acoustic microscope (SLAM) for these investigations.

The SLAM operates at an ultrasonic frequency of 100 MHz and permits assessment of ultrasonic properties of tissue at a microscopic level of resolution (approximately 20  $\mu\text{m}$ ), hence, wound tissue can be easily discerned from wound margins. The SLAM was used to determine ultrasonic speed and attenuation coefficient of normal skin and of maturing wound tissue *in vitro*. We used a canine model to provide wound tissue at various stages of maturation. The data obtained from the SLAM were correlated with accepted standards of wound healing, including histology, collagen biochemistry, and tensile strength testing. The study is unique with regard to the comprehensiveness with which both ultrasound and other tissue properties were characterized. In many ultrasonic tissue characterization studies, published values from the literature for biochemical, mechanical, or morphologic properties are used to estimate material properties. In this study each parameter was determined from the same sample used for ultrasound measurements. We sought to identify ultrasonic features of wounds that might permit the development of a noninvasive instrument capable not only of differentiating wound tissue from normal skin, but also capable of providing objective information

Manuscript received May 5, 1986; accepted for publication October 22, 1986.

This work was supported by National Institutes of Health grant AM21557 and the Rehabilitation Research and Development Service of the Veterans Administration.

Reprint requests to: John Olerud, M.D., Department of Medicine, Division of Dermatology, RM-14, University of Washington, Seattle, Washington 98195.

### Abbreviations:

- ANOVA: multivariate analysis of variance
- DDF: dried, defatted weight
- IL: insertion loss
- MPa: megapascals
- SLAM: scanning laser acoustic microscope

regarding material properties of the tissue such as tensile strength, collagen content, and water content.

### MATERIALS AND METHODS

**Animal Model** Standard paravertebral incised skin wounds, 6 cm in length, were created on 3 adult male mongrel dogs (26–30 kg). The dogs were designated dog A, dog B, and dog C. Wounds were created under sterile, surgical conditions (after the animals were anesthetized with i.v. sodium thiamyl and inhaled halothane) at time points 50, 35, 21, 14, 10, and 7 days before sacrificing the animals. At the time of sacrifice the animals were again anesthetized and wound tissue removed in a manner depicted in Fig 1. In every case, samples were either frozen in liquid nitrogen or placed in fixative according to the protocol for the individual measurements within 5 min of being removed from the animal.

It has been demonstrated that rapid freezing in liquid nitrogen does not affect the mechanical properties of skin and wound tissue [4]. Similarly, Geleskie and Shung observed no differences in ultrasonic impedance among several tissues studied before and after freezing [5]. It was necessary for wound tissue to be frozen in the present study both for transporting specimens and sectioning them for the SLAM, but the study was designed so that all experiments could be accomplished with only 1 cycle of freeze-thaw.

**Tensile Strength** A plastic template 6 cm long and 1.5 cm wide was oriented at right angles to the wound tissue and used to produce properly oriented lines of a standard width and length for excising samples for tensile strength testing (Fig 1). Following normal skin retraction after excision, the samples were approximately 1 cm in width and 5.5 cm in length. To serve as a control for regional variation in tensile strength, adjacent unwounded skin was removed and the skin was cut to the dimensions shown in Fig 1 using a press similar in principle to that previously described [6]. Both wound and control samples were wrapped in aluminum foil, frozen to the temperature of liquid nitrogen, placed in a Ziploc bag, and stored in a Revco freezer at  $-70^{\circ}\text{C}$ . They were subsequently thawed and tested at room temperature on an Instron TT-CM tensile testing machine at a constant rate of 1 cm per min. All samples were evaluated on a single day. The thickness of each specimen was measured by placing it between 2 glass slides and very carefully measuring the thickness of the assembly with a micrometer. The width was then measured, the loading grips were attached, and the specimen was mounted in the testing frame, still at the zero stress length. It was then loaded to failure.

The tensile strength in megapascals (MPa) was calculated by dividing the load at failure by the cross-sectional area of the specimen. The ultimate nominal stress was calculated by dividing the tensile strength of the wound tissue by the tensile strength of the adjacent control. The uncertainty of the measurement is estimated to be  $\pm 6\%$ .

**Biochemistry** Wounds and adjacent skin samples at least 1 cm away from the wound were excised, defatted, wrapped in aluminum foil, frozen in liquid nitrogen, and stored in a Revco freezer at  $-70^{\circ}\text{C}$ . Excess wound margin was removed from wound tissue while viewing the wound under a dissecting microscope. Samples were minced, weighed, dried by lyophilization, and reweighed. The estimated uncertainty in the reported water values is  $\pm 2\%$ . The samples were also defatted at  $4^{\circ}\text{C}$  using chloroform:methanol (2:1) for 18 h followed by methanol extraction for 6 h and reweighed to obtain the dry defatted weight. A 4- to 6-mg aliquot was hydrolyzed in 6 N HCl for determination of total collagen content.

Acetic acid-soluble collagen was extracted from the remainder of the dry defatted tissue by homogenizing the tissue in 0.5 N acetic acid with a tissumizer (Tekmar Corp.) followed by shaking for 18 h at  $4^{\circ}\text{C}$ . The amount of collagen in all cases was measured by hydroxyproline assay using a modified Bergman and Loxley procedure [7]. One sample was assayed 6 times yielding a mean and SD of  $3.94 \pm 0.05$  mg (i.e.,  $\pm 1.3\%$ ).

**Histology** Samples for morphology were trimmed of excessive fat and were immediately placed in half-strength Karnovsky's fixative [8]. Samples were subsequently processed, embedded in Epon 812 [9], and sectioned at a thickness of  $1\ \mu\text{m}$  perpendicular to the plane of the wound and perpendicular to the surface of the skin (Fig 1). Sections were stained with Richardson's stain [10], which differentiates between elastic and collagen fibers.

**Ultrasound Methodology** A  $5 \times 5$  mm sample and a  $5 \times 3$  mm sample (Fig 1) of dog skin with the wound centrally placed were mounted on a circular piece of cork 22 mm in diameter and 3 mm thick. The orientation of the wound axis was marked on the adjacent cork and Ames OCT compound was applied to facilitate cutting frozen sections. The  $5 \times 5$  mm sample was mounted for sectioning parallel to the surface of the skin. The  $5 \times 3$  mm sample was mounted to permit sectioning perpendicular to the skin surface and perpendicular to the plane of the wound. Subsequent discussion will refer to these as "parallel" and "cross-section" sections, respectively. The samples were then frozen in liquid nitrogen, placed in a Ziploc bag, and maintained at the temperature of dry ice while being transported. The samples were air freighted to the Bioacoustics Research Laboratory, Department of Electrical and Computer Engineering at the University of Illinois, Urbana, Illinois where they were then stored in a Revco freezer at  $-70^{\circ}\text{C}$  until evaluation.

Frozen sections 50, 100, and  $150\ \mu\text{m}$  in thickness were obtained from each wound sample by attaching the corks to which the tissue was mounted on the object disk of a Lipshaw Cryostat with Ames OCT compound. Each wound was optically identified in the sections (with the aid of a dissecting microscope when necessary) and the wound margin was trimmed to 0.5 mm on each side of the wound to enable the entire specimen to be viewed in a single field of the SLAM. Samples were on the stage of the SLAM for approximately 30 min during data collection.

Operational details of the SLAM have been published [11–14] and are only summarized here (Fig 2). The SLAM operates in 3 modes. The first mode is similar to a light microscope. Laser light is used to scan, in a raster fashion, a specimen on the microscope stage that has been surrounded by normal saline and covered by a partially mirrored coverslip. Laser light passes through the coverslip and the specimen and subsequently is collected by a photodetector, electronically processed, and transmitted to a television monitor where the optical image is seen (Fig 2C). This optical image is magnified 77 times.

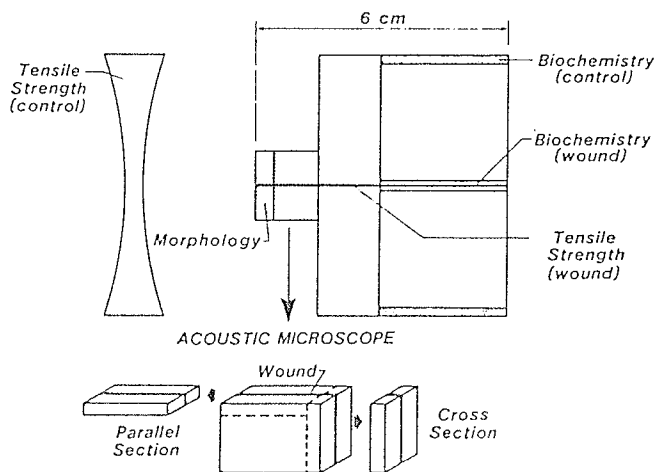
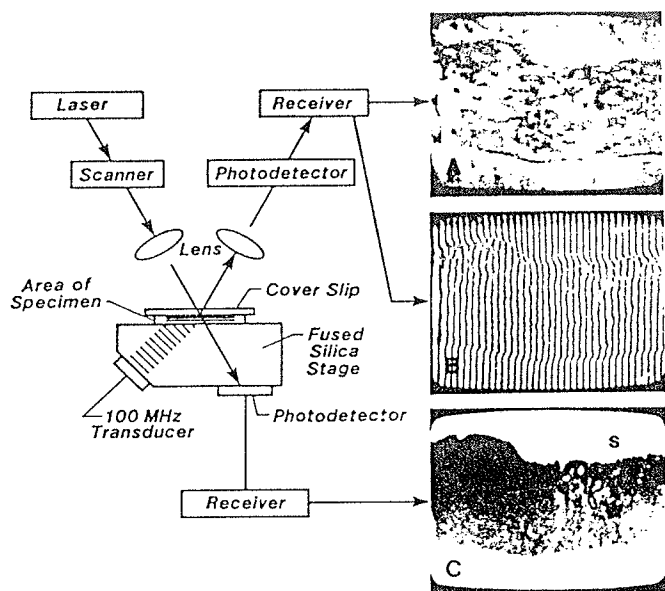


Figure 1. Skin and wound sample allocation. Samples were oriented for both parallel and cross-section analysis by the acoustic microscope.



**Figure 2.** A block diagram of the SLAM. *A*, An example of the acoustic image of a 35-day wound and adjacent skin. This image contains the attenuation coefficient data. The darker areas represent areas of greater acoustic attenuation. *B*, An interferogram from which wave speed is calculated. Speed is calculated from the magnitude of the horizontal shift in the vertical lines. A shift from left to right represents an increase in velocity and vice versa. *C*, An optical image of the unstained frozen section 100  $\mu\text{m}$  thick.

In the second mode, an acoustic image is created by a piezoelectric transducer operating at 100 MHz beneath the microscope stage, transmitting sound waves through the stage, through the specimen under investigation, and subsequently into the partially mirrored coverslip. The acoustic energy incident upon the lower surface of the coverslip thus contains the acoustic image information resulting from the inhomogeneous pathway traversed by the wave in passing through the tissue specimen. Minute disturbances at the lower surface of the coverslip are detected by the scanning laser beam. Since the lower surface of the optically transparent coverslip is partially mirrored, a portion of the laser light is reflected from the surface of the coverslip and collected by a second photodetector. This signal is also electronically processed and displayed on a second television monitor. It represents the acoustic image (Fig 2A). Thus, this instrument is capable of producing simultaneous and real time, acoustic and optical images.

The SLAM also operates in a third mode, the interference mode (Fig 2B). Here, an electronic reference signal is added to the acoustic image signal allowing for determination of the change in phase of the acoustic signal passing through the specimen. That is, the interference mode provides the information necessary to determine, at the microscopic level of structure, variation in speed of propagation of acoustic energy through the specimen under investigation [11].

Speed is calculated from the magnitude of the horizontal shift in the vertical lines (Fig 2B). Note that the interference lines shift to the right as they move from a solution of known ultrasonic speed (saline) into the higher-velocity skin tissue and then back to the left when they reenter the reference solution. The interference image is digitized and stored in a computer. Each interference line is processed by the computer to yield the ultrasonic speed within the region of interest. For each of 3 thicknesses of skin, at least 1, and in some cases 2 or 3, ultrasonic speed determinations were made. All of these speed values are then averaged to yield the ultrasonic speed in meters per second (m/s), reported herein. Considering the uncertainty of measuring the shift in

interference lines and measuring the specimen thickness, the overall uncertainty of the ultrasound speed measurement is  $\pm 1.5\%$  for these heterogeneous specimens [11].

The attenuation coefficient is measured utilizing the insertion loss (IL) method [12], which involves the comparison of 2 signal amplitudes received from the acoustic image, one with and the other without a specimen of known thickness inserted in the sound path. Insertion loss is a logarithmic function of the ratio of these 2 signal amplitudes and provides a quantitative index, in decibels (dB), of the ultrasonic energy loss through the specimen. An IL value is recorded for each of 3 specimen thicknesses. The slope of the IL vs thickness curve, determined by a least squares analysis, yields the attenuation coefficient in dB/mm. The IL measurement sensitivity (minimally detectable change) is 0.2 dB and its precision is  $\pm 5\%$ . Considering the specimen thickness range (50–150  $\mu\text{m}$ ) and the thickness uncertainty ( $\pm 5\%$ ), the final uncertainty of the attenuation coefficient is  $\pm 10\%$  or about  $\pm 5$  dB/mm. However, our data exhibited a greater spread, which is attributed to the highly heterogeneous nature of the specimens.

**Statistical Methods** A standard statistical software package (SPSS) was used to perform analysis of variance and other statistical tests on the data. Statistically significant levels were determined at the 5% level. Linear least squares fit analyses were performed to develop functional relationships between 2 variables such as water vs speed and collagen vs speed. In situations where the relationships appeared to be nonlinear, other fits, such as exponential, log, and power (to fourth order), were also examined. The correlation coefficient,  $r$ , was used in all cases as an indicator of goodness of fit, and was also used as a measure of the percentage of variance in the dependent variable explained by the regression equation. The 2-tailed Student  $t$ -test was used to determine the significance of  $r$ . The F-test for significance of the multivariate analysis of variance (ANOVA) was utilized.

## RESULTS

**Clinical Observations** The weight of dog A remained constant during the study period and dog B gained 2 kg. Dog C had an illness characterized by cough and diarrhea that extended over approximately a 1-month period. At times dog C was given parenteral fluids and antibiotics. No bacterial or viral etiology was diagnosed despite cultures. The symptoms improved significantly during the last 2 weeks of the study period, although the animal lost 2 kg in body weight over the 50-day study period. Clinical observations regarding specific wounds include: in dog A, the day-21 wound had a wound hematoma; in dog B, the day-10 wound had a hemorrhagic crust with slight separation at the surface, the day-50 wound showed some overlap of the margins but appeared otherwise normal; and in dog C, the day-10 wound showed some separation at the surface as a result of the dog chewing out 3 stitches.

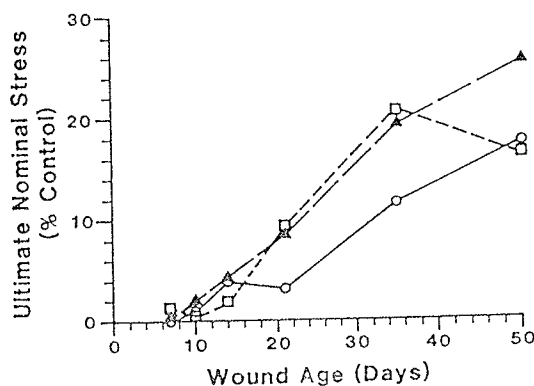


**Figure 3.** Wound tensile strength plotted as a percent of adjacent normal skin. Dog A, open circles; Dog B, open squares; Dog C, solid triangles.

Table I. Ultrasonic and Biochemical Data From the Wounds and Control Skin of Three Dogs

	Wound Age (days)	Percent H <sub>2</sub> O	Total Collagen (% wet weight)	Total Collagen (% DDF weight) <sup>a</sup>	Percent Acid-Soluble Collagen (as % of total)	Tensile Strength (MPa)	Ultrasonic Attenuation Coefficient (dB/mm)		Ultrasonic Speed (m/s)		
							Parallel	X-Sec	Parallel	X-Sec	
Dog A	Skin	7	65	18	68	4	39.2	84.7	60.1	1655	1622
		10	61	18	76	2	28.5	33.9	47.7	1615	1618
		14	60	23	71	2	31.7	66.9	36.8	1646	1636
		21	61	21	73	4	27.4	44.1	45.0	1622	1607
		35	56	25	70	2	31.7	51.6	75.5	1623	1631
	50	60	22	71	1	38.1	62.0	51.0	1650	1598	
	Wound	7	65	12	48	3	0.01	—	—	—	—
		10	76	15	65	3	0.28	24.6	27.3	1554	1554
		14	48	23	65	6	1.25	31.5	22.0	1583	1532
		21	—	—	67	9	0.86	33.6	36.2	1532	1547
35		66	14	60	11	3.66	43.3	75.0	1580	1598	
50	60	21	64	7	6.67	38.6	37.0	1578	1576		
Dog B	Skin	7	65	24	80	2	46.7	34.6	38.5	1635	1630
		10	65	21	72	2	49.0	33.5	31.1	1608	1635
		14	62	23	77	2	37.3	26.5	41.8	1662	1657
		21	63	25	77	3	47.2	11.8	43.0	1624	1610
		35	63	25	80	2	49.6	52.9	64.7	1656	1639
	50	64	23	79	1	39.9	63.2	41.1	1625	1696	
	Wound	7	73	12	57	2	0.55	25.0	17.8	1562	1538
		10	76	10	51	3	0.16	25.3	16.2	1478	1542
		14	74	13	65	2	0.71	16.4	32.8	1571	1553
		21	73	14	65	5	4.33	10.0	17.0	1574	1552
35		71	16	68	7	10.10	15.7	—	1582	1596	
50	68	16	68	3	6.45	48.6	35.1	1576	1613		
Dog C	Skin	7	60	25	73	5	30.6	38.0	83.7	1624	1701
		10	59	22	70	6	27.7	44.5	44.2	1618	1609
		14	61	21	71	6	22.0	41.6	48.6	1582	1610
		21	59	24	74	5	27.9	41.1	41.6	1633	1622
		35	59	25	74	3	37.5	36.3	46.8	1657	1612
	50	60	24	69	4	33.3	50.3	47.2	1655	1608	
	Wound	7	66	12	42	6	0.04	15.3	32.5	1560	1560
		10	69	12	50	5	0.54	30.9	28.0	1553	1543
		14	68	12	46	7	0.82	19.4	31.5	1555	1522
		21	73	14	60	10	2.35	25.2	33.3	1562	1554
35		69	20	67	—	7.23	32.4	34.9	1550	1564	
50	69	16	61	16	8.43	—	30.8	1607	1590		

<sup>a</sup>DDF weight = dry, defatted weight.

**Tensile Strength** In general, there was a progressive increment in the relative wound strength as the duration of the repair process increased (Fig 3, Table I). Exceptions were noted in the case of 3 wounds that had been noted to be clinically abnormal before tensile strength testing (i.e., dog B, days 10 and 50 and dog A, day 21). In Fig 3 the results of wound tensile strength tests are reported as a percent of the adjacent control skin. The tensile strength (MPa) of the control samples were as follows: dog A,  $32.8 \pm 4.9$  (mean  $\pm$  SD); dog B,  $45.0 \pm 5.1$ ; dog C,  $29.9 \pm 5.3$ .

**Biochemical Analysis** Table I summarizes the biochemical analyses performed on the wound and control skin tissues. Total collagen in every case was lower for wound tissue compared with control skin and was lowest at the earlier stages of healing, days 7 and 10. The values for total collagen appeared to increase as the wound matured and the difference between wound and control skin appeared to decrease as wounds matured. Acetic acid-soluble collagen, which is a measure of the newly synthesized, less cross-linked collagen, generally rose above control levels by day 14 and it was 2–5 times higher than control levels on days, 21, 35, and

50. The water content was generally higher in wound tissue than in control tissue.

**Histology** Morphologic evidence of normal wound repair was documented by light microscopy as illustrated in Fig 4. An increase in the amount of collagen with time was noted as was an increase in fiber bundle size.

**Ultrasound Results** Data from the parallel and cross sections from each of the 3 dogs are presented in Table I. The ultrasonic propagation properties of skin specimens were quite heterogeneous, i.e., the specimen to specimen variations were considerable. These variations tended to be most evident in the acoustic images which, in turn, influenced the attenuation coefficient values.

An ANOVA was performed to determine the effects of various factors on the speed values [13]. There was no significant variation due to specimen thickness (50, 100, or 150  $\mu$ m) or section type (parallel or cross section). In addition, there were no significant variations explained as a result of using 3 different dogs. This indicated that the data for all 3 dogs, for all 3 specimen thicknesses,

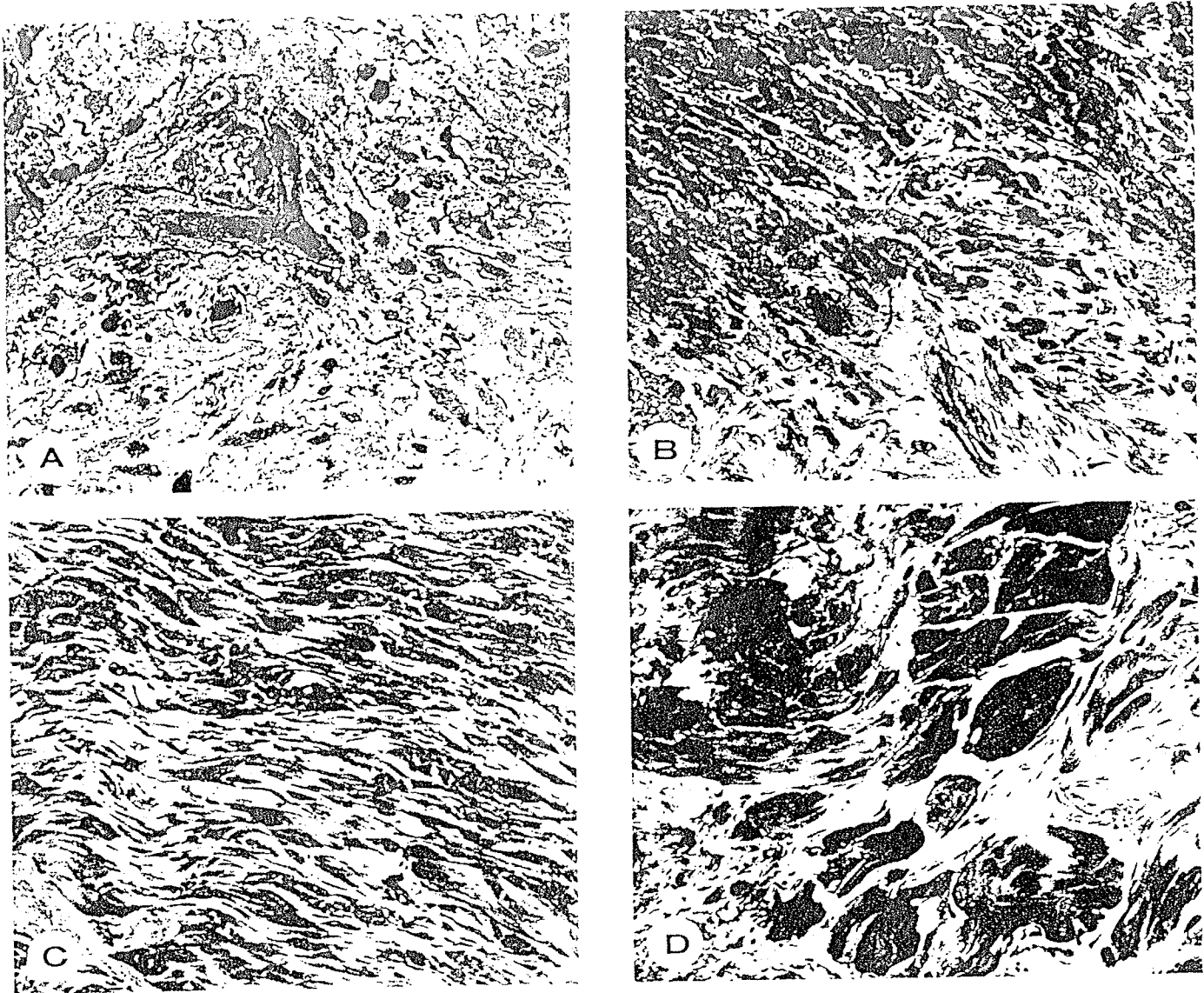


Figure 4. Photomicrographs of canine wound connective tissue and control. An array of normal canine dermal collagen is depicted in (D) ( $\times 330$ ). Compare this with the scanty and thin collagen fibers and highly cellular connective tissue in the 7-day-old wound (A). In the 21-day (B) and the 50-day (C) wounds there are a greater number of collagen fibers, a more orderly alignment of fiber bundles, and they are more densely packed.

and for parallel and cross-section sections could be pooled for analysis without affecting the speed results. The greatest amount of variance in speed was explained by whether the specimen came from wound or the adjacent skin. The differences between these 2 tissue types were significant ( $p < 0.001$ ) as determined by a *t*-test.

To determine whether wound age had a significant effect for both wound and skin, a separate ANOVA was performed for each of these tissue types. The data for all dogs, sections, and thicknesses were again combined. Wound age had a marginal effect on the variance in ultrasonic speed for adjacent skin ( $p = 0.050$ ) with 7% of the speed variation explained by wound age. The percentage of speed variation explained by age in the wound was greater (28%) and it was highly significant ( $p < 0.001$ ). Although the ANOVA results cannot say whether speed changed monotonically as a function of wound age, the results suggested that ultrasonic speed measurements reflected the wound healing process. In addition, it appeared that whatever changes were oc-

curing in the wound were also occurring, although to a lesser extent, in the unwounded adjacent skin (Fig 5).

Determination of the attenuation coefficient yielded only one value per specimen of a given age and section type. A Student's *t*-test for comparison of sample means was performed to determine whether the attenuation coefficient was dependent on the section type. For both skin and wound tissue, there were no significant differences between the attenuation coefficients for parallel and cross sections. Hence, the results for all dogs and sections could also be combined for analysis. With the combined data, an ANOVA could be done to determine the effect of wound age on the attenuation coefficient in skin and wound. In contrast to the speed results, the effect of wound age was not significant with either skin or wound. This was most likely due to the more limited attenuation coefficient data available (only 6 attenuation coefficient values per wound age vs 19-32 speed values per wound age), and to the greater overall variance with attenuation coefficient values (Fig 5).

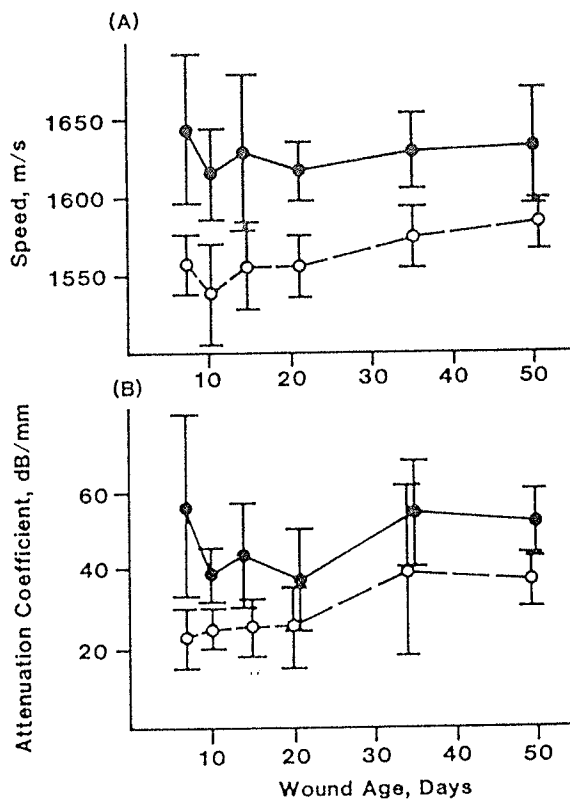


Figure 5. Plots of ultrasonic attenuation coefficient and ultrasonic speed as a function of wound age for wound (open circles) and adjacent skin (solid circles) tissue. The mean and SD of values for the three dogs are plotted.

To better characterize the relationship between the ultrasonic parameters and the traditional wound healing indicators, speed and attenuation coefficient results were correlated with the collagen, water, and tensile strength of both wound and adjacent skin. The ultrasonic speed and attenuation coefficient decreased as the tissue water concentration increased, and increased as the tissue total collagen content increased (Figs 6, 7). Ultrasonic speed was highly correlated with both total collagen (as a percentage of wet weight) and with percent water (Table II). The correlation between attenuation coefficient and both collagen and water was less dramatic, as is shown by the greater range of the 95% confidence interval (Figs 6, 7), but was still highly significant ( $p < 0.001$ ) (Table II).

Table III. Wound Tissue: Significant Linear Correlations Between Ultrasonic Speed (c) and Collagen and Tensile Strength Results

Variables	Regression Equation	r	Significance
Speed, m/s vs:			
Collagen, % wet weight (CW)	$c = 3.05 CW + 1516$	0.49	0.027
Collagen, % DDF weight* (CD)	$c = 1.29 CD + 1483$	0.47	0.028
Tensile strength, MPa (TS)	$c = 4.69 TS + 1546$	0.71	< 0.001

\*DDF weight = dry, defatted weight.

When collagen content was calculated as a percentage of dried, defatted weight (DDF), the best relationship with speed was non-linear (fourth order), ( $r = 0.81$ ,  $p < 0.001$ ), whereas for attenuation coefficient, the best relationship was linear ( $r = 0.46$ ,  $p = 0.003$ ). Both speed and attenuation coefficient were highly correlated with wound and skin tissue tensile strength (Table II).

Using data for the wound tissue alone, significant linear correlations were determined between speed and both collagen (total and DDF) and tensile strength (Table III). Ultrasonic speed was significantly correlated with all measurements of collagen content and strongly correlated with tensile strength. No significant correlations between the wound attenuation coefficient and tensile strength, collagen, or water content were observed, however. Again, this may be explained by the large measurement of uncertainty associated with the attenuation coefficient and the limited number of values. With the values for wound tissue alone, at least one of the ultrasonic parameters—speed—was strongly related to wound strength. As mentioned above, when data for both wound and skin were combined, and thus the range of values extended, both ultrasound parameters were more highly correlated with tensile strength, collagen, and water content.

## DISCUSSION

Animal studies using classic methodologies have permitted much information to be compiled about various stages of wound healing. Temporal sequences relative to wound strength, wound morphology, and dynamics of certain biochemical events are well described [1,6,15–18]. In the present study we have documented the normal progression of wound maturation in a canine model using tensile strength measurements, light microscopy, and collagen biochemistry. Those properties were related to the acoustical properties of the same samples. Thus, with normal wound maturation there was an increase in tensile strength and an increase in ultrasonic attenuation coefficient and wave speed.

Total collagen measurements in each animal showed that the

Table II. Wound and Adjacent Skin: Significant Best Fit Correlations Between Ultrasonic Speed (c) or Attenuation Coefficient (A) and Biochemical and Tensile Strength Results

Variables	Regression Equation	r	Significance Level
Speed, m/s vs:			
% Water (W)	$c = -3.73 W + 1840$	-0.57	< 0.001
Collagen, % wet weight (CW)	$c = 6.73 CW + 1470$	0.80	< 0.001
Collagen, % DDF weight* (CD)	$c = 0.33 \times 10^{-5} (CD)^4 + 1525$	0.81	< 0.001
Tensile strength, MPa (TS)	$c = 24.34 (TS)^{0.4} + 1529$	0.90	< 0.001
Attenuation coefficient, dB/mm vs:			
% Water (W)	$A = -1.77 (W) + 154$	-0.73	< 0.001
Collagen, % wet weight (CW)	$A = 1.68 CW + 6.61$	0.56	< 0.001
Collagen, % DDF weight (CD)	$A = 0.72 CD - 9.41$	0.46	0.003
Tensile strength, MPa (TS)	$A = 0.47 TS + 29.1$	0.58	< 0.001

\*DDF weight = dry, defatted weight.



hydroxyproline measured in wound samples was always less than comparable measurements in normal surrounding skin. Values for total collagen in wounds were lowest at 7 days after wounding. They reached a plateau and remained relatively level until day 50. Our inability to document a more progressive accumulation of total wound collagen in general may reflect the technical difficulty in separating new wound collagen from the preexisting collagen at wound margins. We believe the acid-soluble collagen more accurately reflects the change in wound collagen since it is less cross-linked, and hence, more acid soluble than the preexisting collagen at the wound margins. The expected rise in acid-soluble collagen between the 1st and 5th weeks of wound repair was observed. The decrease in acid-soluble collagen at day 50 observed in 2 of the animals perhaps reflects an increase in cross-linking of the newly formed wound collagen. An increase in the collagen fiber bundle size seen by light microscopy in the day-50 wounds supports this conclusion as does the general increase in wound tensile strength.

The ultrasonic propagation properties of tissues; namely attenuation coefficient and wave speed, are thought to be determined at the level of large molecules. In blood, for example, the ultrasonic absorption coefficient is directly proportional to the protein concentration, whether the protein is in solution or contained within cells [19,20]. Similar observations have been made for liver [21]. In skin the major protein is collagen and its concentration in skin is significantly affected by the water content of the tissue.

Tissue water content influences the propagation properties of ultrasound. The ultrasonic attenuation in an infant brain was approximately one-third that of an adult brain [22], which reflects the much higher water content in the infant brain (approximately 90%), as compared with adult brain (76-79%) [23]. Likewise, the ultrasonic attenuation of an adult hydrocephalic brain [22], and an edematous brain [23] are less than that of normal adult brain [24]. The speed of sound in fetal brain from the 16th day of gestation to term increases with age from 1513 to 1540 m/s [25]. We made similar observations in this study regarding an increase in ultrasonic attenuation and speed with a decrease in water content in skin and wounds.

Collagen plays an important role in the ultrasonic propagation properties of tissues for several reasons. One reason is that collagen is a high-tensile strength, insoluble fiber found in most connective tissues, including skin, cartilage, tendon, bone, and muscles. In the skin, collagen is the main structural component constituting 65-75% of the DDF. In addition, collagen exhibits acoustical properties widely different from those of the other common tissue constituents [26,27]. For example, collagenous fibers exhibit a static elastic modulus (Young's modulus) approximately 1000 times greater than that of other tissues [26]. Since ultrasonic speed is proportional to the square root of the elastic modulus, the ultrasonic speed is expected to be significantly greater for collagen than for other constituents. Direct measurements of ultrasonic velocity in tendon threads support this concept [27,28]. The higher ultrasonic speed in collagen implies that collagen also has a higher characteristic acoustic impedance. This, in turn, implies that there will be an impedance mismatch between collagen and surrounding tissue, and that collagen is therefore responsible for much of the reflection and scattering that occurs within tissues. Thus, it is reasonable to hypothesize [26] that collagen is largely responsible for the echo patterns that permit soft tissues to be visualized when ultrasound is used for imaging [26,29].

The ultrasonic attenuation coefficient in infarcted vs normal myocardium has been measured [30]. There was an increase in the attenuation coefficient with increasing collagen concentration during scar formation. The initially low attenuation coefficient may have been related not only to the low collagen content but also to an increase in water content of the tissue following myocardial injury, and the subsequent inflammatory response before myocardial repair and scar formation.

In an earlier study [31], we characterized cutaneous wound

tissue using a scanning laser acoustic microscope and showed that there was an increase in the ultrasonic speed and a suggestion of an increase in the ultrasonic attenuation coefficient coincident with an increase in the age of scar tissue. Significant improvements in the data collection and analysis system were applied in the present study [11,12]. These improvements permit quantitative assessment of the ultrasonic attenuation coefficient as well as a quantitative analysis of speed for each skin and wound sample.

In the present study a linear relationship between ultrasonic speed and collagen content (% wet weight) was established. A similar logarithmic relationship could equally have been determined. The linear relationship derived in *Results* and a logarithmic relationship yielded approximately the same fit. Mathematically stated, the logarithmic relationship demonstrated is: collagen (% wet weight) =  $-1113 + 153 \ln$  [ultrasonic speed (m/s)]. An earlier literature survey analysis of speed vs collagen content for a composite of 8 biologic tissues (skin not included) representing collagen contents from 0-10% wet weight showed a strong ( $r = 0.95$ ) nonlinear relationship [30] to be as follows: collagen (% wet weight) =  $-1700 + 230 \ln$  [ultrasonic speed (m/s)]. These two equations are nearly identical. The slope and intercept constants are just scaled by a factor of 1.5. This suggests an element of agreement between the earlier literature survey, in which relationships between ultrasonic properties and collagen were deduced and the empirically derived relationships observed in the present study. In addition, the agreement between these two separately derived equations indicates that the results of the present study may extend far beyond the scope of this study to other soft tissues as well.

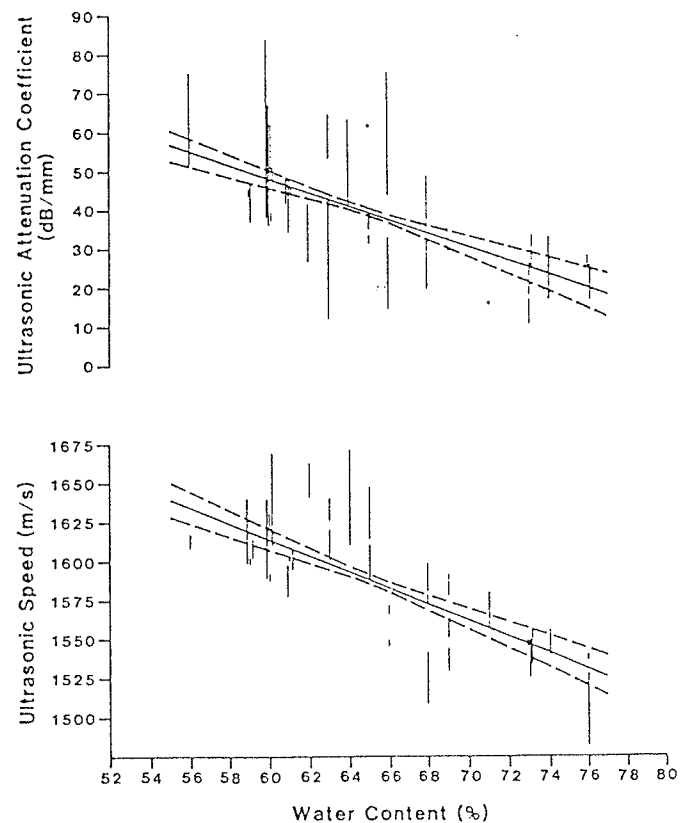


Figure 6. Plots of the least squares fit for the relationship of tissue water content for skin and wound samples as a function of attenuation coefficient (upper panel) and ultrasonic speed (lower panel). Vertical lines connect 2 data values, one from the parallel sections of a given skin or wound specimen, the other from the cross section. The 95% confidence intervals are plotted for each of the least-squares fit lines. The fits are significant  $p < 0.05$ .

Figure 7 relates the ultrasonic attenuation coefficient and ultrasonic speed to the percentage of tissue collagen regardless of whether the tissue is skin or wound. These data clearly demonstrate a significant linear functional relationship in which the attenuation coefficient and wave speed both increase with increasing tissue collagen content. Figure 6, likewise, shows a significant linear inverse relationship between ultrasonic attenuation coefficient and speed with tissue water content. Although these relationships have been postulated previously, this is, to our knowledge, the first clear experimental demonstration of these relationships where ultrasound velocity and attenuation coefficient as well as collagen and water measurements were obtained in the same specimen.

Tensile strength is perhaps the most important property of a wound from the perspective of a surgeon involved in patient care. Since wound tensile strength relates most directly to collagen content and configuration, one would expect to see a relationship between tensile strength and wave speed as well as attenuation coefficient because both of the ultrasound parameters correlated with collagen content in the present study. A highly significant relationship was measured between ultrasonic speed and tensile strength of the wound tissue, but the relationship between tensile strength and attenuation coefficient did not reach statistical significance for wound tissue alone. This may be because of the

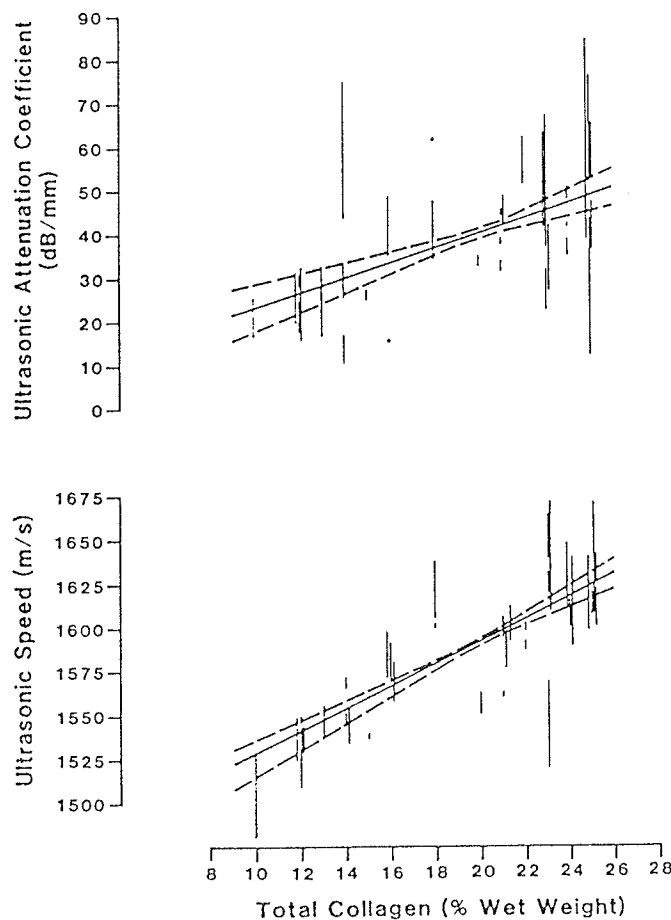


Figure 7. Plots of the least squares fit for the relationship of tissue collagen content of skin and wound samples as a function of attenuation coefficient (upper panel) and ultrasonic speed (lower panel). Vertical lines represent 2 data values, one from the parallel section of a given skin or wound specimen, the other from the cross section. The 95% confidence intervals are plotted for each of the least-squares fit lines. The fits are significant ( $p < 0.05$ ).

relatively small number of samples studied and the fact that most of the wound ages selected in our study had relatively little tensile strength compared with normal skin. Nonetheless, these data show the feasibility of using ultrasound measurements to obtain information from tissue regarding material properties such as tensile strength and collagen content. Ultrasound measurements in the present study were done *in vitro*; however, it is possible in the future to design instruments capable of making ultrasound measurements useful for these purposes *in vivo*.

While the ultrasonic parameters used in the present study allow clear differentiation of wound tissue from normal skin, they do not appear to permit differentiations between earlier wounds and later wounds in the 7- to 21-day time period which are most relevant for clinical purposes. There was, however, a consistent trend toward an increase in ultrasonic speed and attenuation coefficient with an increase in wound maturation. We will examine these clinically important time points with larger numbers of samples in future studies and will consider the use of other ultrasound modalities in the future, which may more clearly define differences in wound maturation.

In this study we have attempted to characterize the interactions of ultrasound with normal skin as well as healing wounds. The wound model provides an opportunity to observe changes in ultrasonic propagation properties in tissue as changes occur in water content and tensile strength, as well as the quantity and configuration of collagen. Such basic studies relating ultrasound properties to tissue material properties may provide important insights in the design of instrumentation capable of noninvasive and quantitative assessment of normal and pathologic processes of the skin.

*The authors would like to acknowledge the valuable assistance of Nancy Higgins and Diane McCarthy in manuscript preparation, and Dr. Jackie Bickenbach for collaboration regarding sample handling and tissue processing.*

#### REFERENCES

1. Peacock EE, VanWinkle W: The biochemistry and the environment of wounds and their relationship to wound strength, in *Surgery and Biology of Wound Repair*. Philadelphia, WB Saunders, 1970, pp 129-170
2. deVlieger M, Holmes JH, Kazner E, Kossoff G, Kratochwil A, Kraus R, Poujol J, Strandness DE (Eds): *Handbook for Clinical Ultrasound*. New York, John Wiley & Son, 1978
3. Dines KA, Sheets PW, Brink JA, Hanke CW, Condra KA, Clendenon JL, Goss SA, Smith DJ, Franklin TD: High frequency ultrasonic imaging of skin: experimental results. *Ultrasonic Imaging* 6:408-434, 1984
4. Marangoni RD, Glaser AA, Must JS, Brody GS, Beckwith TG, Walker GR, White WL: Effect of storage and handling techniques on skin tissue properties. *Ann NY Acad Sci* 136:439-454, 1966
5. Geleskie JV, Shung KK: Further studies on acoustic impedance of major bovine blood vessel walls. *J Acoust Soc Am* 71:467-470, 1982
6. Levenson SM, Crowley LV, Greever EF, Rosen H, Berard CW: Studies of wound healing: experimental method, same effect of ascorbic acid and effect of deuterium oxide. *J Trauma* 4:543-566, 1964
7. Bergman I, Loxley R: Two improved and simplified methods for the spectrophotometric determination of hydroxyproline. *Anal Chem* 35:1961-1965, 1963
8. Karnovsky MJ: A formaldehyde-glutaraldehyde fixative of high osmolarity for use in electron microscopy. *J Cell Biol* 27:137A, 1965
9. Luft JH: Improvements in epoxy resin embedding methods. *Journal of Biophysical and Biochemical Cytology* 9:409-414, 1961
10. Richardson KC, Jarrett L, Finke EH: Embedding in epoxy resins for ultrathin sectioning in electron microscopy. *Stain Technol* 35:313, 1960
11. Embree PR, Tervola KMU, Foster SG, O'Brien WD Jr: Spatial



- distribution of the speed of sounding biological materials with the scanning laser acoustic microscope. *IEEE Trans Son Ultrason* SU-32:341-350, 1985
12. Tervola KMU, Foster SG, O'Brien WD Jr: Attenuation coefficient measurement technique at 100 MHz with the scanning laser acoustic microscope. *IEEE Trans Son Ultrason* SU-32:259-265, 1985
  13. Steiger DL: Ultrasonic assessment of skin and wounds with the scanning laser acoustic microscope. MS thesis, University of Illinois, Urbana, 1986
  14. Tervola KMU, Gummer MA, Erdman JW, O'Brien WD Jr: Ultrasonic attenuation and velocity properties in rat liver as a function of fat concentration: a study at 100 MHz using a scanning laser acoustic microscope. *J Acoust Soc Am* 77:307-313, 1985
  15. Viljanto J: Tensile strength of healing wounds, in *Biophysical Properties of the Skin, Treatise of the Skin*, vol. 1. Edited by HR Elden. New York, Wiley-Interscience, 1971, p 452-483
  16. Ross R, Odland GF: Fine structure observations of human skin wounds and fibrogenesis, in *Repair and Regeneration*. Edited by JE Dumphy, W VanWinkle. New York, McGraw-Hill, 1969, pp 101-115
  17. Madden JW, Peacock EE: Studies on the biology of collagen during wound healing. I: Rate of collagen synthesis and deposition in cutaneous wounds of the rat. *Surgery* 64:288-294, 1968
  18. Madden JW, Peacock EE: Studies on the biology of collagen during wound healing. III: Dynamic metabolism of scar collagen and remodeling of dermal wounds. *Am Surg* 174:511-520, 1971
  19. Carstensen EL, Li K, Schwan HP: Determination of the acoustic properties of blood and its components. *J Acoust Soc Am* 25:286-289, 1953
  20. Carstensen EL, Schwan HP: Acoustic properties of hemoglobin solutions. *J Acoust Soc Am* 31:305-309, 1959
  21. Pauly H, Schwan HP: Mechanism of absorption of ultrasound in liver tissue. *J Acoust Soc Am* 50:692-699, 1971
  22. Kremkau FW, McGraw CP, Barnes RW: Acoustic properties of normal and abnormal human brain, in *Ultrasonic Tissue Characterization II*. Edited by M Linzer. NBS Publication 525. Washington, DC, U.S. Government Printing Office, 1979, pp 81-84
  23. Altman PL, Dittmer DS: *Blood and Other Body Fluids*. Washington, DC, Federation of American Societies for Experimental Biology, 1961
  24. Oka M, Yosioka K: Ultrasonic absorption of human brain tissue. Presented at First World Federation for Ultrasound in Medicine and Biology, paper no. 1302, San Francisco, 1976
  25. Waldimiroff JW, Craft IL, Talbert DC: *In vitro* measurements of sound velocity in human fetal brain tissue. *Ultrasound Med Biol* 1:377-382, 1975
  26. Fields S, Dunn F: Correlation of echographic visualizability of tissue with biological compositions and physiological state. *J Acoust Soc Am* 54:809-812, 1973
  27. Goss SA, O'Brien WD Jr: Direct ultrasonic velocity measurements of mammalian collagen threads. *J Acoust Soc Am* 65:507-511, 1979
  28. O'Brien WD Jr: The relationship between collagen and ultrasonic attenuation and velocity in tissue. *Proceedings of Ultrasonics International '77* (IPC Science and Technology Press, Ltd., Guildford, England), 1977, pp 194-205
  29. Pohlhammer J, O'Brien WD Jr: Dependence of the ultrasonic scatter coefficient on collagen concentration in mammalian tissues. *J Acoust Soc Am* 69:283-285, 1981
  30. O'Donnell M, Mimb JW, Miller JG: The relationship between collagen and ultrasonic attenuation in myocardial tissue. *J Acoust Soc Am* 65:512-517, 1979
  31. O'Brien WD Jr, Olerud JE, Shung KK, Reid JM: Quantitative acoustical assessment of wound maturation with acoustic microscopy. *J Acoust Soc Am* 69:575-579, 1981
  32. Johnson RL, Goss SA, Maynard VA, Brady JK, Frizzell LA, O'Brien WD Jr, Dunn F: Elements of tissue characterization, Part I, Ultrasonic propagation properties, in *Ultrasonic Tissue Characterization II*. Edited by M Linzer. NBS Publication 525. Washington, DC, U.S. Government Printing Office, 1979, pp 19-27